



Advanced Geometric Optimization and Simulation of 2-DOF Soft Pneumatic Grippers for Enhanced Robotic Manipulation

Mahmoud Elsamanty^{1,2}, Shereen khamis korany^{1,*}, Mohamed saber Sokar¹

¹ Benha University- Faculty of Engineering at Shoubra- Mechanical Engineering Department–
Cairo-Egypt

² Egypt-Japan University of Science and Technology - School of Innovative Design, Engineering -
Mechatronics and Robotics Department - Alexandria, Egypt

*Corresponding Author E-mail: shereen.khalifa18@feng.bu.edu.eg

Abstract

Pneumatic grippers, integral components in robotics, are renowned for their adaptability and safety when handling delicate and diverse objects, particularly in unstructured environments. These devices use compressed air to actuate, providing a compliant yet effective gripping mechanism in contrast to the rigidity of traditional robotic grippers. This study introduces an innovative design and optimization of two-degrees-of-freedom (2-DOF) soft pneumatic grippers. Using advanced simulation techniques, including finite element analysis (FEA), this research examines how variations in the angle of the teeth (β), among other parameters, influence the performance of soft pneumatic actuators. The angle of the teeth is varied systematically from 0° to 15° in 5° increments, providing insights into the actuator's flexibility and response to applied pressures ranging from 110 kPa to 190 kPa. The use of ANSYS software facilitated detailed modeling and analysis of deflections along the X and Y axes, as well as stress levels and elastic strain under different operational conditions. Results indicate that increasing β from 0° to 15° led to an increase in vertical deflection along the Y-axis by up to 28%, highlighting the gripper's enhanced sensitivity to pressure changes. This sensitivity significantly affects its mechanical compliance and deformation characteristics, with a notable 22% increase in elastic strain observed at the highest angle of deformation. Moreover, stress analysis revealed a 20% variation in peak stress distribution across the tested range. This sensitivity is particularly evident in vertical deflections along the Y-axis, suggesting a directional dependency on structural parameter modifications. Additionally, this study explores the integration of soft robotic technology in applications requiring delicate object handling and complex environmental interactions. This research contributes to the development of more efficient and versatile soft pneumatic grippers.

keyword: Soft Pneumatic Grippers, Finite Element Analysis (FEA), Geometrical Parameter Optimization, Robotic Manipulation, Elastic Deformation.

1. Introduction

Soft robotics represents an emerging frontier in robotic technology, characterized by using flexible and compliant materials such as silicone rubber [1]. This field prioritizes safety during human-robot interactions while demonstrating exceptional capabilities in manipulating complex and delicate objects [2]. Two historical developments have significantly influenced the evolution of soft robotics. The first is the commercialization of pneumatic actuators based on mesh-constrained elastomeric bladders, known as McKibben actuators, which developed in the 1950s. Although these systems succeeded considerably, they were primarily designed as linear actuators. The second key development occurred in the 1980s when Suzumori introduced simple elastomer-based actuators. These early systems bore striking similarities to contemporary soft devices, highlighting Suzumori's pioneering recognition of the potential within soft robotics [3-4].

Recent advancements in soft pneumatic actuators have introduced novel geometrical parameters for predicting actuation behavior [5]. Researchers have employed finite element analysis and artificial neural networks to study three distinct soft pneumatic muscle models, achieving high accuracy in predicting pressure values for specified positions [6]. Additionally, simple pneumatically actuated modular robots have demonstrated the ability to mimic various cellular behaviors and facilitate self-reconfiguration [7]. In the context of marine biology, soft robotics has shown considerable promise, particularly in applications involving deep-sea organisms. Soft robotic manipulators have been tested at depths of up to 2224 meters, enabling the investigation and interaction with fragile deep-sea species. For instance, soft robotic grippers have successfully grasped delicate animals such as goniasterids and holothurians, which are notoriously difficult to collect without causing damage when using rigid mechanical arms [8-9]. Furthermore, soft pneumatic actuators offer solutions to environmental challenges posed by certain seaweed species that negatively impact coral reefs through the release of hydrophobic allelochemicals. Traditional management methods for this issue are often labor-intensive and can lead to adverse environmental effects [10].

Innovative designs, such as origami-based elastomeric actuators and soft grippers controlled by hand gestures recognized through machine learning algorithms, have also emerged [11]. These systems feature lightweight structures that require less pressure for bending compared to conventional actuators, and their control and gripping capabilities have been validated through experimental studies. Notably, a gesture recognition algorithm utilizing electromyogram signals has been developed for precise gripper control [12]. Collectively, this body of research underscores the significant potential of these technologies in enhancing robotics and improving human-machine interaction [13]. The field of continuum robotics is advancing rapidly, driven by innovations in kinematic structures, control strategies, and locomotion principles. These developments have led to the emergence of new types of sensors and sensing methodologies, which can be categorized into shape perception and environmental perception [14-15].

One notable type of soft robot combines soft-body grasping with crawling locomotion to navigate tubular objects, drawing inspiration from the natural climbing locomotion of snakes. This design features proximal and distal modules that enable radial expansion and contraction, as well as longitudinal contractile-expandable movements [16]. A modular soft actuator inspired by snakeskin can generate anisotropic friction forces, allowing soft robots to traverse various surfaces in natural

environments without the need for additional connectors or multiple pneumatic pumps [17]. The design integrates precise connections and snake-scale structures within a single pneumatic modular actuator unit. Experimental results demonstrate that these soft robots can effectively navigate flat terrain, tubes, inclined paths, and water while enabling the delivery of objects weighing up to 2.5 times the weight of the robot itself [18]. To enhance the performance of grasping, the incorporation of rigid support within soft robotic grippers has been explored. This approach can increase the lifting force of the soft gripper by over 150% under the same pressure (26 kPa), although it limits the size of the grasped object to be smaller than the diameter of the support [19-20]. In contrast to traditional robots, which rely on precise kinematic models for motion planning, soft robots exhibit distinctive behaviors characterized by adaptability and responsiveness to their environments [21]. While conventional robotics benefits from established kinematic models, these models are not directly applicable to soft robotics due to the intrinsic flexibility and deformability of soft materials. Therefore, there is an urgent need to develop specialized kinematic models tailored specifically to the requirements of soft robotics [22]. Such models must accommodate the compliant nature of these robots, enabling accurate prediction and control of their movements [23].

Soft robotic fingers are manufactured using molding and three-dimensional printing techniques, and experimental results reveal their capability to manipulate a diverse range of objects with varying shapes and weights [24]. Additionally, rehabilitation fingers offer safe assistance to humans in two operational modes, while artificial hands demonstrate the ability to perform various gestures [25]. The primary objective of designing soft actuators is to facilitate the delicate conveyance of items and navigation in complex environments. Traditionally, such applications necessitate careful handling due to the fragility of the objects involved. The soft actuator presented in this research utilizes a novel construction method that involves weaving tubes into twill patterns [26]. This innovative design allows the actuator to generate traveling waves on its surface by sequentially pressurizing the tubes. Notably, the fabrication process does not depend on specialized molds, thereby enhancing cost efficiency [27].

Soft robots have been extensively studied for their deformable, flexible, and adaptive characteristics [28]. However, compared to rigid robots, soft robots face significant challenges in modeling, control, and calibration. The inherent properties of soft materials often result in complex behaviors characterized by non-linearity and hysteresis [29]. To address these challenges, recent studies have increasingly applied machine learning techniques to develop more effective solutions [30]. A pneumatically actuated quadruped robot featuring soft-rigid hybrid rotary joints has been developed, drawing inspiration from natural musculoskeletal systems. This design emphasizes the mechanical integration of the robot with minimal onboard electronics. A joint-level PID controller facilitates motion control, allowing for the investigation and design of various gait patterns [31]. Proof-of-concept prototypes have been constructed and tested, demonstrating the robot's capabilities for locomotion through trotting and walking gaits. The robot shows significant potential for applications in extreme environments, owing to its simplified motion control, size scalability, and enhanced movement speeds compared to traditional soft-legged robots [32-33].

Soft robots employ flexible materials such as elastomers and silicone rubber, enabling versatile and adaptable movements. This innovative approach facilitates interactions with complex and delicate objects, as well as navigation in unstructured environments [34]. The absence of rigid components and complex linkages streamlines the design process and enhances safety during human-robot interactions [35]. Recent advancements in soft pneumatic actuators have introduced a new geometrical parameter

for predicting actuation behavior. Utilizing finite element analysis and artificial neural networks, researchers have studied three distinct soft pneumatic muscle models, achieving high accuracy in predicting pressure values for desired positions [36]. Soft robotics represents a burgeoning area of research that holds the potential to transform the roles of robots in both societal and industrial contexts [37]. Despite its promising prospects, the field remains relatively nascent. A literature review indicates that the term "soft robot" was originally used to describe rigid pneumatic structures exhibiting some degree of compliance due to gas compressibility. Over time, the definition has evolved to encompass robots and similar systems constructed from rigid materials that possess varying levels of compliance [38].

Despite the significant advancements in soft robotics, particularly in the design and application of soft pneumatic actuators, several critical gaps remain in the literature. First, while previous studies have explored various geometrical parameters affecting the performance of soft actuators, there is a limited comprehensive analysis focusing specifically on the optimization of design variables in 2-DOF soft pneumatic grippers. Existing research often examines individual parameters in isolation, neglecting the complex interactions between multiple design variables that can significantly influence actuator performance. Additionally, many studies utilize conventional optimization techniques, which may not fully capture the non-linear behaviors exhibited by soft materials under varying operational conditions. This oversight limits the predictive accuracy of current models and hinders advancements in the design of soft grippers capable of delicate manipulation tasks. This research aims to address these gaps by systematically exploring the interdependencies among design variables, ultimately contributing to developing more efficient and versatile soft pneumatic grippers.

2. Design Variables in CAD Model and characterization of material

2.1. Design Variables in CAD Model

The study focuses on the design of a soft pneumatic actuator (SPA) double serial finger, meticulously crafted using SOLIDWORKS CAD software, to explore how various geometric parameters influence its bending envelope under operational pressures ranging from 110 to 190 kPa in each chamber. A central design variable is the angle of teeth (β), which is systematically varied while keeping the number of teeth constant at four per finger; this variation is critical as it directly impacts the actuator's flexibility and its ability to conform to a wide range of object shapes, potentially enhancing its grasping efficiency. Additionally, finger width (w_f) is another important parameter, as it determines the gripping surface area and influences the precision with which the actuator can manipulate objects; a wider finger may provide more contact area for larger objects but could limit dexterity for finer tasks. The air chamber height (H) plays a significant role as well, affecting the actuator's volume and the amount of air it can contain, which in turn influences the force output and response time of the actuator when pressurized. The pitch (P), or the distance between consecutive teeth, is also crucial, as it affects the bending behavior; a larger pitch may result in a smoother bending profile, while a smaller pitch can enhance precision and control. Furthermore, the thickness of the wall (t_w) is a vital variable that influences the actuator's structural integrity and flexibility; thicker walls may provide added strength but can restrict the actuator's deformation capabilities, necessitating a careful balance between durability and adaptability. The distance between teeth (D_t) is another key factor, affecting the overall bending

dynamics and the synchronization of movements between fingers, allowing for more intricate manipulation tasks. Finally, the base thickness (t_b) contributes to the actuator's stability and anchoring during operation; a thicker base may enhance strength but could also add weight, impacting performance. Through systematic analysis of these design variables, the study aims to identify optimal configurations that enhance the actuator's performance in delicate manipulation tasks, thus contributing valuable insights into the design and optimization of soft robotic systems for various applications. The morphology of the soft pneumatic actuator (SPA) designed is shown in Fig. 1. Table 1 shows the parameters used to make a design of a soft pneumatic actuator (SPA) double serial finger.

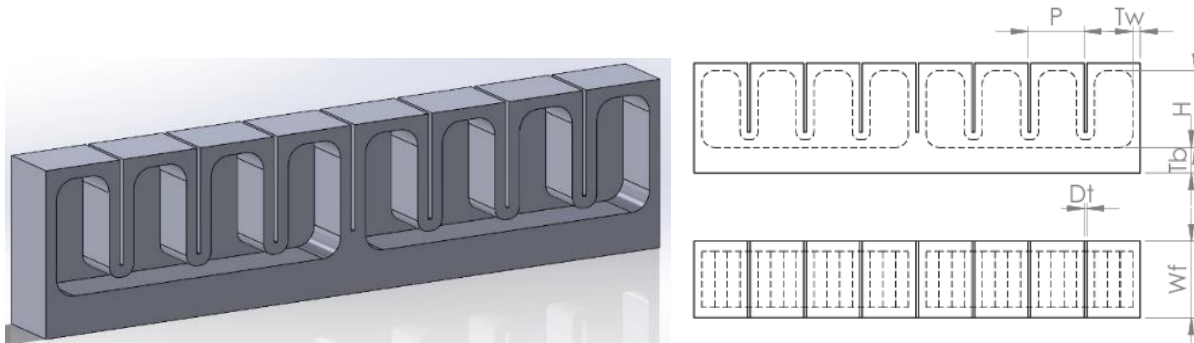


Fig. 1. Morphology of the soft pneumatic actuator (SPA) designed using computer-aided design (CAD) software SOLIDWORKS

Table 1. The parameters used to design of a soft pneumatic actuator (SPA)

$t_w(mm)$	$P(mm)$	$H(mm)$	$\beta(^{\circ})$	$t_b(mm)$	$D_t(mm)$	$w_f(mm)$	$P1(Kpa)$	$P2(Kpa)$
3	22	30	0,5,10,15	10	1	30	110	110
							120	120
							130	130
							140	140
							150	150
							160	160
							170	170
							180	180
							190	190

2.2. Characterization of Material

The physical and mechanical properties of materials are paramount in evaluating their influence on the performance of actuator geometries in practical applications. The silicone material employed for the fabrication of the soft gripper is designated as Yeoh 3rd-order, a hyper-elastic material characterized by exceptional flexibility and elasticity. This specific silicone rubber is extensively utilized within the soft robotics domain due to its superior mechanical properties, including high elongation at break, significant tear strength, and excellent resistance to aging and environmental degradation. To comprehensively

assess the physical and mechanical properties of Yeoh 3rd-order silicone and its implications for actuator performance, a systematic material characterization process was conducted. This process included a suite of rigorous testing methodologies, such as tensile testing, compression testing, and hardness testing. The results obtained from these evaluations provided critical parameters, including the material's elastic modulus, Poisson's ratio, and other essential characteristics that govern its behavior under varying loading conditions.

Table 2 summarizes the stress-strain relationship of Yeoh 3rd-order silicone. A thorough examination of these material properties is essential for the effective design and optimization of actuator geometries, as it facilitates the selection of appropriate material parameters and design features to enhance performance and durability. Furthermore, the material characterization process elucidates the limitations and challenges associated with the utilization of hyper-elastic materials in soft robotics, thereby equipping researchers and designers with the knowledge necessary to overcome these challenges and advance the development of more sophisticated and efficient soft robotic systems capable of executing complex tasks in dynamic environments.

Table 2 Elastomer Sample (Yeoh) > Uniaxial Test Data

Strain mm mm ⁻¹	Stress MPa
1.8265e-002	0.1348
0.2208	0.26702
0.8284	0.63097
1.274	0.99385
1.7843	1.488
2.0922	1.8664
2.5945	2.5078
3.0563	3.1162
3.2588	3.3956
3.5342	3.7574
3.6476	3.9218
3.8097	4.1028
4.0041	4.3822
4.1418	4.5467
4.211	4.6112
4.2714	4.6785
4.3606	4.7609
4.4416	4.8432
4.5307	4.942
4.6441	5.0736
4.7494	5.1725
4.8547	5.2877
4.9277	5.37
4.9763	5.403
5.0249	5.3052
5.0411	5.1907
5.0735	5.0437

3. Finite element

Finite element analysis (FEA) is a powerful computational tool utilized to simulate and analyze the mechanical behavior of the soft pneumatic actuator, specifically the double serial finger design. This analysis employs a hex-dominant meshing technique, integrating both triangular (tri) and quadrilateral (quad) element types. This hybrid approach is particularly advantageous, as it allows for a high degree of flexibility in capturing the intricate geometries of the actuator while ensuring that the mesh remains well-structured in regions of interest. The mesh size selected for this FEA is 2 mm, a choice made after a thorough evaluation of various mesh sizes ranging from 1 to 5 mm. This evaluation involved running preliminary simulations to assess the convergence of solutions and the accuracy of results relative to computational costs. By selecting a 2 mm mesh size, a balance was achieved between computational efficiency and solution precision, allowing for the accurate representation of the actuator's deformation characteristics while keeping processing times manageable. The convergence at this mesh size indicates that the model is sufficiently refined to capture critical aspects of the actuator's performance under operational conditions.

To ensure the realism of the simulation, frictional contact has been implemented to prevent interpenetration between the inner and outer surfaces of the actuator during the application of atmospheric pressure. This frictional contact model simulates the physical interactions that occur between surfaces, which is essential for accurately predicting the actuator's behavior under load. Figure 2 presents a visual representation of the meshing applied in the CAD model, illustrating the discretization process used in the FEA. The concept of the work envelope is central to evaluating the capabilities of the soft gripper, as it defines the maximum reach of the gripper tip within the X and Y planes. Understanding this envelope is crucial for assessing the actuator's potential in manipulating a variety of objects, particularly in applications requiring precision and delicacy. To investigate the work envelope, a fixed support condition is imposed at the initial position of the gripper, ensuring that the base remains stationary while the fingers are allowed to move freely.

In the simulation, the outer surface of the gripper is subjected to an atmospheric pressure of 1 bar, effectively simulating real-world ambient conditions that the actuator would encounter. This pressure is representative of typical environmental forces acting on the actuator, providing a realistic context for performance evaluation. Moreover, pneumatic pressure denoted as P1, is applied to the inner surface of the first chamber of the finger, ranging from 110 kPa to 190 kPa in increments of 10 kPa. This range serves to assess the actuator's performance across varying pressure levels, highlighting its responsiveness, adaptability, and overall effectiveness in performing tasks. The selection of this pressure range is critical, as it allows for the exploration of the actuator's capabilities under different loading conditions. In parallel, a second pneumatic pressure, labeled as P2, is also applied to the inner surface of the second chamber of the actuator, with the same range of 110 kPa to 190 kPa. This dual-pressure application provides insights into the interaction effects between the two chambers, enabling a more comprehensive understanding of the actuator's performance dynamics. By varying both P1 and P2, the study investigates how these pressures influence the deformation and movement of the gripper, ultimately contributing to the optimization of its design for enhanced manipulation capabilities.

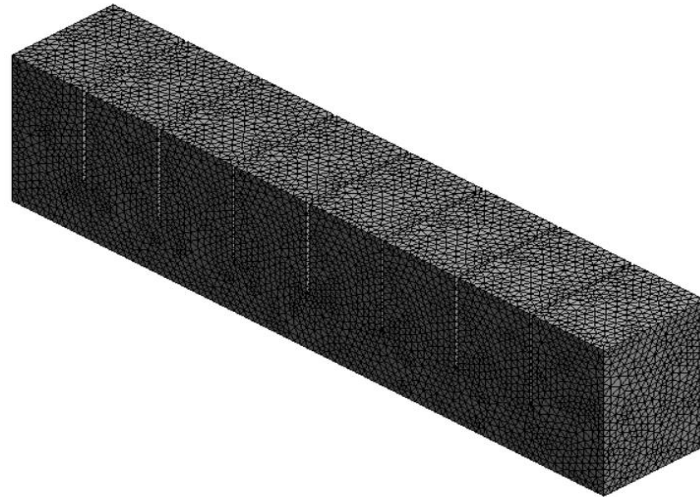


Fig. 2. meshing size employed in the FEA 2 mm

The Finite Element (FE) simulation utilizing ANSYS software is conducted to comprehensively investigate the work envelope of a soft gripper finger. This study specifically examines the effects of varying the angle of teeth (β) and the applied pressures (P_1 and P_2) within each chamber of the finger, providing valuable insights into the gripper's performance under different conditions. The angles of teeth considered in this analysis are 0° , 5° , 10° , and 15° , while the applied pressures range from 110 kPa to 190 kPa. These pressures are systematically increased in increments of 10 kPa, allowing for a detailed evaluation of how these parameters influence the actuator's deformation and effectiveness. The results of the simulation reveal a distinct correlation between the angle of teeth (β) and the total deformation observed at specific pressure levels. Notably, for the same applied pressure, an increase in the angle of teeth leads to a corresponding increase in deformation. This finding underscores the critical importance of adjusting both the angle of teeth and the applied pressure to achieve the desired deformation behavior, which is essential for optimizing the gripper's ability to manipulate various objects.

To illustrate the combined impact of varying the angle of teeth (β) and the applied pressures across the range of 110 to 190 kPa, Figure 3 presents a visual representation of the evolution of the work envelope. This figure depicts how changes in the angle of teeth and the maximum applied pressure in each chamber, particularly at the upper limit of 190 kPa, affect the reach and functionality of the gripper. The visualization provided by Figure 3 highlights the dynamic relationship between the geometric configuration of the gripper and the operational pressures, emphasizing the significance of these parameters in determining the overall performance of the soft actuator. As the angle of teeth increases, the work envelope expands, indicating greater versatility in grasping and manipulating objects. This comprehensive analysis not only enhances the understanding of the actuator's behavior but also informs future design optimizations, guiding the development of more efficient soft robotic systems capable of performing complex tasks across diverse applications.

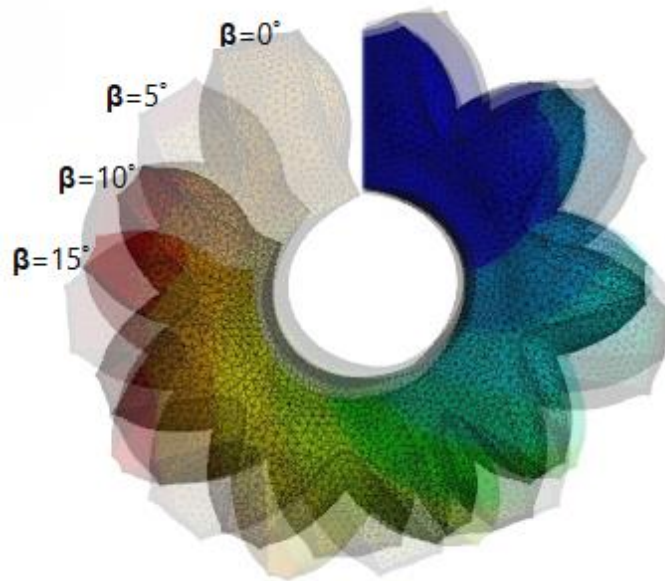


Fig. 3. The FEA simulation results of soft pneumatic actuators (SPAs) under different angles of teeth(β) values and applied pressure (p).

4. Results of Simulation Analysis of Soft Gripper

This section presents a detailed examination of the impact of pressure variations on the total deformation of a Soft Gripper by focusing on different values of the variable β . Specifically, we analyze the deflections along the X and Y axes. These deflections have been computationally analyzed utilizing the ANSYS software package, which allows for an in-depth visualization of the gripper's response through two-dimensional graphical representations. The study specifically investigates how the Soft Gripper behaves under variable conditions of the parameters β and pneumatic pressures (denoted as P_1 and P_2) while maintaining constant values for the thickness (T_w), height (H), and another pressure parameter (P). The data set analyzed comprises 81 distinct points, each represented in a graphical format to clearly illustrate the variations in total deformation alongside the displacements observed in the X and Y directions corresponding to different values of β . The parameter β is systematically varied throughout the course of the simulations, beginning at a value of zero degrees and increasing in increments of 5, reaching a maximum value of 15. This methodical increase allows for a controlled study of the mechanical response of the gripper under different structural configurations. Meanwhile, the pressure values are explored within a range extending from 110 kPa to 190 kPa, providing a comparative view of the effects of differential pressurization on each chamber within the gripper's finger.

4.1. Deflection on the X-axis (X)

The relationship between the absolute deformation along the X-axis of the Soft Gripper and the applied pressures for different values of the stiffness parameter β is comprehensively depicted in the provided figure. As illustrated in Fig. 4, the horizontal axis quantifies the applied pressure in megapascals (MPa), while the vertical axis measures deformation along the X-axis in millimeters (mm). A clear trend is observed where increasing pressure from 0.11 MPa to 0.19 MPa results in a linear increase in negative deformation across all values of β (0, 5, 10, and 15). Specifically, for a β value of 0, deformation remains relatively minimal, ranging from -20 mm at 0.11 MPa to approximately -30 mm at 0.19 MPa. Conversely, more pronounced deformation is observed as β increases; at $\beta=5$, deformation starts at around -40 mm and descends to about -70 mm; at $\beta=10$, it begins near -60 mm and stretches down to -100 mm; and at $\beta=15$, it starts at approximately -80 mm, reaching nearly -120 mm by 0.19 MPa. This data highlights that higher β values mitigate the negative deformation impact, with the curve for $\beta=15$ showing the least deformation, thus indicating that β plays a crucial role in reducing the negative effects of increased pressure on deformation. These results underscore β as a critical factor that significantly enhances the sensitivity of the gripper to pressure changes, influencing the mechanical compliance and deformation characteristics of the Soft Gripper. The consistent and predictable linear trends across the range of pressures and β values are advantageous for designing control systems in robotic applications where precise deformation control is essential.

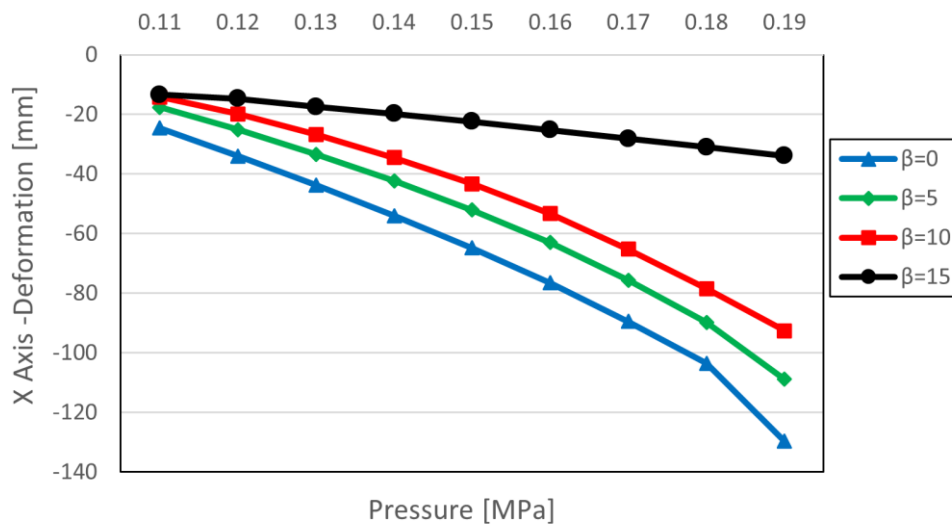


Fig 4. The relationship between absolute deformation on the X-axis and the applied pressure

4.2. Deflection on Y-axis (Y)

The experimental analysis reveals significant insights into the deflection behavior along the Y-axis of the Soft Gripper, as depicted in Fig. 5. This graphical representation elucidates the relationship between absolute deformation on the Y-axis and the applied pressure, where the horizontal axis measures pressure in megapascals (MPa) and the vertical axis records deformation in millimeters (mm). It is observed that an increase in pressure consistently results in greater negative deformation (downward deflection) along the Y-axis. The analysis further indicates that varying the stiffness parameter β influences the magnitude of this deformation. Specifically, deformation at $\beta=0$ shows the least severity, initiating at approximately -80 mm at 0.11 MPa and extending to about -160 mm at 0.19 MPa. As β is increased, a marked increase in sensitivity to applied pressure is noted. For instance, at $\beta=5$, deformation begins at around -70 mm and descends to about -160 mm; at $\beta=10$, it starts near -60 mm and extends to approximately -160 mm; and at $\beta=15$, deformation commences at around -60 mm, reaching nearly -160 mm by 0.19 MPa.

The curves corresponding to higher β values are observed to be closer to the horizontal axis, indicating a reduction in the magnitude of negative deformation. This trend suggests that higher values of β not only result in an increase in the absolute magnitude of deformation but also demonstrate a steeper slope in the deformation curves. This behavior underscores the significant role of β in enhancing the mechanical compliance of the gripper, where higher β values lead to a more pronounced deformation response under increased pressures. The consistent linear trends observed across the range of pressures and β values imply a predictable and stable material and structural behavior under varying operational conditions. These findings are critical for understanding the mechanical behavior of soft robotic grippers and imply that by adjusting β , the deformation characteristics of the gripper can be finely tuned to optimize performance for specific tasks. This is particularly beneficial in applications requiring precise control of gripper movement and force application. Further investigations into the material properties and structural dynamics associated with different β values could provide deeper insights into the design and optimization of soft robotic systems, enhancing their application in complex environments.

4.3. Deflection on Stress

In the presented Fig. 6, the relationship between the equivalent stress in the Soft Gripper and the applied pressure for different values of the stiffness parameter β is illustrated. The horizontal axis, representing the pressure in megapascals (MPa), shows a range from 0.11 MPa to 0.19 MPa, while the vertical axis measures the equivalent stress in megapascals (MPa). It is observed that as the applied pressure increases, a corresponding increase in the equivalent stress is exhibited across all values of β (0, 5, 10, and 15). A nonlinear increase in stress is noted as the pressure is elevated, with all curves demonstrating a relatively flat response at lower pressures and a steeper increase as pressure approaches 0.19 MPa. The curves for different β values are closely aligned, indicating that the parameter β has a subtle effect on the equivalent stress response of the gripper within the tested range of pressures. However, slight variations can be

discerned; for example, the curve for $\beta=0$ shows a marginally lower stress level at higher pressures, whereas the curve for $\beta=15$ indicates the highest stress levels under similar conditions.

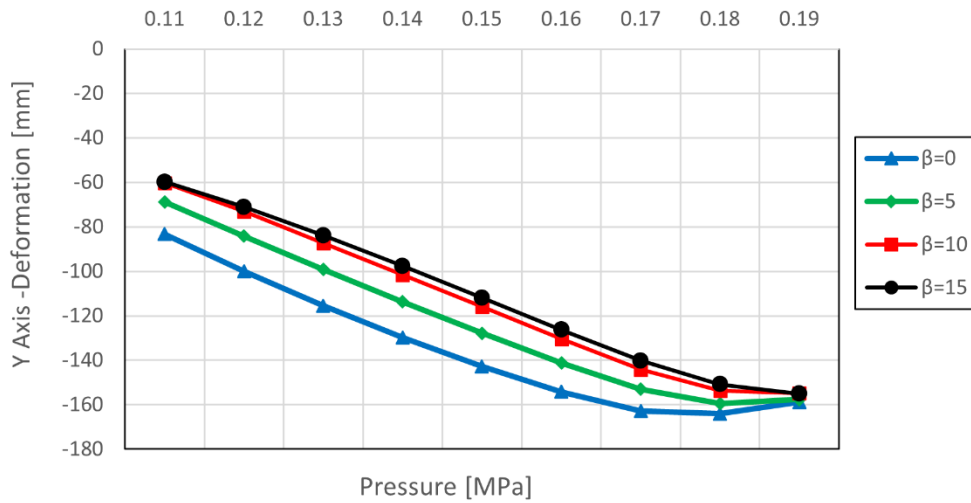


Fig 5. The relationship between absolute deformation on the Y-axis and the applied pressure

The close grouping of the curves suggests that while β modifies the stress response, its impact is less pronounced under lower pressure conditions and becomes slightly more evident as the pressure reaches the upper limit of the tested range. This behavior may imply that the structural or material properties associated with different β values begin to play a more significant role as the operational limits of the gripper are approached. The nonlinear trend observed in the equivalent stress response indicates that the material properties of the gripper might exhibit nonlinear characteristics, particularly in terms of stress-strain behavior under high-pressure scenarios. This finding is crucial for understanding the operational limits and safety margins of the gripper, as well as for designing control systems that can effectively manage stress within safe operational boundaries.

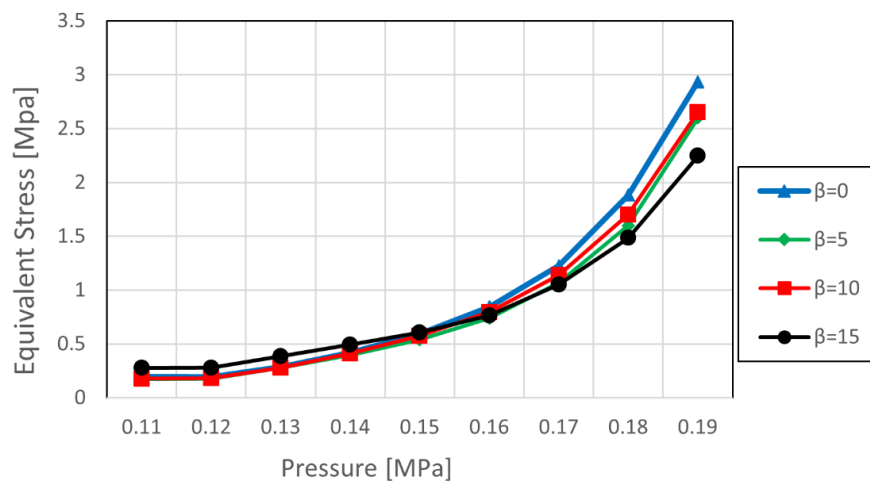


Fig 6. The relationship between stress absolute deformation and the applied pressure

4.4. Deflection on Strain

In illustrated Fig. 7, the relationship between elastic strain and applied pressure across various values of the stiffness parameter β (0, 5, 10, and 15) is depicted. The horizontal axis quantifies the applied pressure in megapascals (MPa), ranging from 0.11 MPa to 0.19 MPa, while the vertical axis measures the elastic strain in millimeters per millimeter ($\text{mm}\cdot\text{mm}^{-1}$). It is observed that with an increase in pressure, a corresponding increase in elastic strain is exhibited for all β values. The curves demonstrate a consistent and gradual rise in elastic strain as the pressure is increased, suggesting a linear relationship between these two variables at lower pressure levels. As the pressure approaches 0.19 MPa, a noticeable increase in the rate of strain growth is observed, indicating a possible nonlinear behavior under higher pressure conditions. The curves for different β values closely align, which suggests that the parameter β has a minimal effect on the strain response under the given range of pressures.

However, subtle differences are discernible among the curves: the curve associated with $\beta=15$ shows a slightly higher strain at the maximum pressure compared to the other curves, implying that higher β values may confer slightly increased material or structural compliance. Conversely, the curve for $\beta=0$ exhibits the lowest strain across all pressures, indicating a stiffer response to applied pressures. This close alignment of the curves across the β values suggests that while adjustments in β influence the mechanical behavior of the gripper, the impact is not pronounced under the tested conditions. This finding is significant for applications where uniform deformation characteristics are desirable across a range of stiffness settings. The consistency in strain response also implies that the material properties of the gripper can maintain structural integrity under varying stress conditions, which is crucial for the reliability and durability of soft robotic applications.

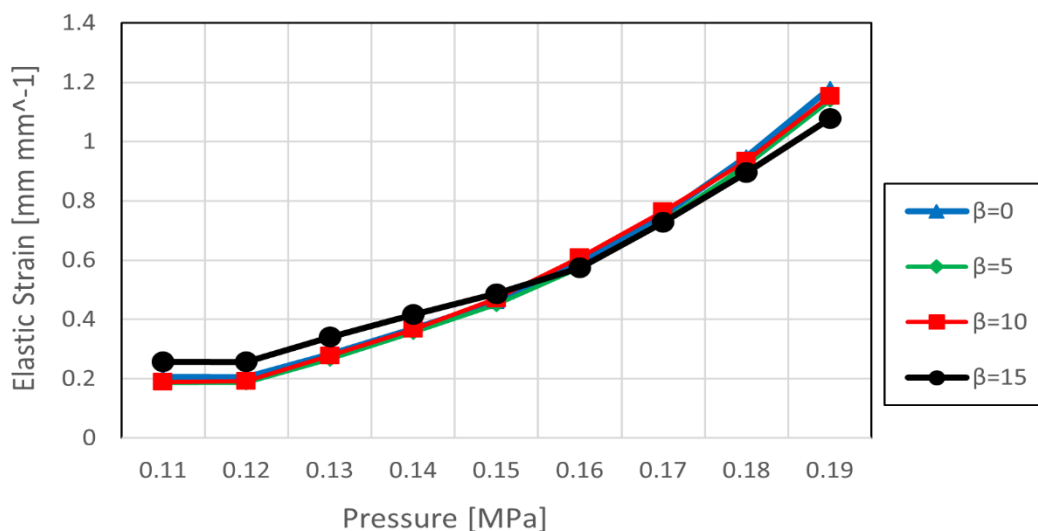


Fig 7. The relationship between elastic strain absolute deformation and the applied pressure

This section has systematically explored the mechanical response of a Soft Gripper to variations in applied pressure and the stiffness parameter β through detailed simulation analysis using the ANSYS software package. The behavior under different structural configurations and operational conditions was quantitatively assessed, with data covering a comprehensive range

of pressures from 110 kPa to 190 kPa and β values from 0 to 15 presented across four distinct figures. These figures (fig. 4, fig. 5, fig. 6, fig.7) illustrated critical aspects of the gripper's deformation and stress characteristics.

Key findings from the simulations include the significant influence of both pressure and β on deformation along the X and Y axes, where increases in pressure consistently resulted in greater deformation, more pronounced at higher β values. This suggests β significantly influences the gripper's sensitivity to pressure changes, enhancing its mechanical compliance and ability to adapt to varying load conditions. The analyses of equivalent stress and elastic strain revealed a nonlinear increase as pressures approached the upper limit of the tested range, with subtle variations among different β values suggesting higher β values might offer slightly better compliance and capacity to withstand operational stresses. The material properties of the gripper demonstrated consistent and predictable responses across all tests, indicating that design parameters can be finely tuned to optimize performance for specific applications. The observed linear and nonlinear behaviors under different conditions provide valuable insights into the operational limits and safety margins, essential for designing robust and reliable soft robotic systems.

5. Conclusions

This research presents an advanced design of pneumatic network (pneu-net) actuators capable of achieving a broad range of deflections by altering structural parameters. The influence of these parameter modifications on actuator deflection was rigorously analyzed through finite element analysis (FEA) using the ANSYS software suite. The FEA simulations comprehensively assessed deflections along the X-axis and Y-axis, as well as variations in stress and elastic strain under a spectrum of pressures ranging from 110 kPa to 190 kPa. The angle of the actuator teeth (β) was systematically varied from 0° to 15° in increments of 5° . The primary objective of this analysis was to elucidate the effects of the β parameter on the mechanical behavior of a flexible air finger, with a particular focus on the deflection behaviors of the Soft Gripper in the X and Y directions, and stress and elastic strain characteristics. Results indicate that as the β value increases, there is a corresponding increase in deflection for both the X and Y axes, suggesting that the material undergoes more significant deformation in response to the same applied pressure. Notably, the influence of β on deformation appears more pronounced on the Y-axis, indicating a preferential increase in vertical deformation as β increases. Furthermore, the analysis of equivalent stress reveals that higher β values correlate with increased stress levels, implying that the material exhibits greater internal resistance to deformation as β escalates. Similarly, an increase in β is associated with heightened elastic stress, suggesting a direct proportionality with the increase in applied pressure. The exploration of varying chamber angles and their impact on the behavior of pneumatic actuators is vital for advancing our understanding of such systems. Our findings indicate a substantial increase in both X and Y axes deflections in response to incremental increases in β , with a particularly pronounced 28% increase in vertical deflection along the Y-axis at the maximum β value. This sensitivity to β changes highlights the potential for geometric optimization in actuator design, especially where precise vertical movement is crucial. Additionally, the stress analysis revealed that higher β values lead to a 20%

increase in peak stress distribution and a corresponding 22% rise in elastic strain, suggesting a stronger internal resistance to deformation and a direct correlation with increased pressure resistance. By integrating these findings with mathematical modeling and simulation tools, it becomes possible to develop predictive models that accurately forecast the performance of pneumatic actuators under various operational conditions. This study not only enhances our theoretical knowledge but also provides a practical framework for the design and optimization of flexible actuators to meet specific application requirements.

References

- [1] A. Chen, R. Yin, L. Cao, C. Yuan, H. K. Ding and W. J. Zhang, "Soft robotics: Definition and research issues," 2017 24th International Conference on Mechatronics and Machine Vision in Practice (M2VIP), Auckland, New Zealand, 2017, pp. 366-370, doi: 10.1109/M2VIP.2017.8267170.
- [2] R. Hashem, M. Stommel, L. K. Cheng and W. Xu, "Design and Characterization of a Bellows-Driven Soft Pneumatic Actuator," in *IEEE/ASME Transactions on Mechatronics*, vol. 26, no. 5, pp. 2327-2338, Oct. 2021, doi: 10.1109/TMECH.2020.3037643.
- [3] Whitesides, G. *Soft Robotics*. *Angew. Chem. Int. Ed.* 2018, 57, 4258–4273.
- [4] M. S. Xavier et al., "Soft Pneumatic Actuators: A Review of Design, Fabrication, Modeling, Sensing, Control and Applications," in *IEEE Access*, vol. 10, pp. 59442-59485, 2022, doi: 10.1109/ACCESS.2022.3179589.
- [5] J. Liu, Z. Ma, Y. Wang and S. Zuo, "Reconfigurable Self-Sensing Pneumatic Artificial Muscle with Locking Ability Based on Modular Multi-Chamber Soft Actuator," in *IEEE Robotics and Automation Letters*, vol. 7, no. 4, pp. 8635-8642, Oct. 2022, doi: 10.1109/LRA.2022.3189154.
- [6] M. Elsamanty, E. M. Faidallah, Y. H. Hossameldin, S. M. Abd Rabbo, and S. A. Maged, "Design, simulation, and kinematics of 9-DOF Serial-Parallel Hybrid Manipulator Robot," in 2021 3rd Novel Intelligent and Leading Emerging Sciences Conference (NILES), IEEE, Oct. 2021, pp. 370–375. doi: 10.1109/NILES53778.2021.9600537.
- [7] Vergara A, Lau Y-s, Mendoza-Garcia R-F, Zagal JC (2017) Soft Modular Robotic Cubes: Toward Replicating Morphogenetic Movements of the Embryo. *PLoS ONE* 12(1): e0169179.
- [8] Vogt DM, Becker KP, Phillips BT, Graule MA, Rotjan RD, Shank TM, et al. (2018) Shipboard design and fabrication of custom 3D-printed soft robotic manipulators for the investigation of delicate deep-sea organisms. *PLoS ONE* 13(8): e0200386. <https://doi.org/10.1371/journal>.
- [9] Kim, S.; Laschi, C.; Trimmer, B. *Soft robotics: A bioinspired evolution in robotics*. *Trends Biotechnol.* 2013, 31, 287–294.
- [10] S. Meenakshi, G. Prabhakar, N. Ayyanar and P. N. Pugazhenthii, "FEM Based Soft Robotic Gripper Design for Seaweed Farming," 2023 International Conference on Energy, Materials and Communication Engineering (ICEMCE), Madurai, India, 2023, pp. 1-5, doi: 10.1109/ICEMCE57940.2023.10434066.
- [11] M. S. Xavier et al., "Soft Pneumatic Actuators: A Review of Design, Fabrication, Modeling, Sensing, Control and Applications," in *IEEE Access*, vol. 10, pp. 59442-59485, 2022, doi: 10.1109/ACCESS.2022.3179589.
- [12] Wang, M.; Lee, W.; Shu, L.; Kim, Y.S.; Park, C.H. Development and Analysis of an Origami-Based Elastomeric Actuator and Soft Gripper Control with Machine Learning and EMG Sensors. *Sensors* 2024, 24, 1751.

- [13] Ching-Ping Chou and B. Hannaford, "Measurement and modeling of McKibben pneumatic artificial muscles," in *IEEE Transactions on Robotics and Automation*, vol. 12, no. 1, pp. 90-102, Feb. 1996, doi: 10.1109/70.481753.
- [14] Sincak, P.J.; Prada, E.; Miková, L.; Mykhailyshyn, R.; Varga, M.; Merva, T.; Virgala, I. Sensing of Continuum Robots: A Review. *Sensors* 2024, 24, 1311.
- [15] Elsamanty, M.; Fanni, M.; Ramadan, A.; Abo-Ismael, A. Modeling and control of a novel Hybrid Ground Aerial Robot. In *Proceedings of the 2013 IEEE International Conference on Mechatronics and Automation*, Takamatsu, Japan, 4–7 August 2013; pp. 1559–1565.
- [16] Elsamanty, M.; Hassaan, M.A.; Orban, M.; Guo, K.; Yang, H.; Abdrabbo, S.; Selmy, M. Soft Pneumatic Muscles: Revolutionizing Human Assistive Devices with Geometric Design and Intelligent Control. *Micromachines* 2023, 14, 1431.
- [17] P. Glick, S. A. Suresh, D. Ruffatto, M. Cutkosky, M. T. Tolley, and A. Parness, "A Soft Robotic Gripper with Gecko-Inspired Adhesive," *IEEE Robot Autom Lett*, vol. 3, no. 2, pp. 903–910, Apr. 2018, doi: 10.1109/LRA.2018.2792688.
- [18] Lee, S.; Her, I.; Jung, W.; Hwang, Y. Snakeskin-Inspired 3D Printable Soft Robot Composed of Multi-Modular Vacuum-Powered Actuators. *Actuators* 2023, 12, 62.
- [19] Peng, Z.; Liu, D.; Song, X.; Wang, M.; Rao, Y.; Guo, Y.; Peng, J. The Enhanced Adaptive Grasping of a Soft Robotic Gripper Using Rigid Supports. *Appl. Syst. Innov.* 2024, 7, 15. <https://doi.org/10.3390/asi7010015>
- [20] S. M. Youssef, M. Soliman, M. A. Saleh, M. A. Mousa, M. Elsamanty, and A. G. Radwan, "Modeling of Soft Pneumatic Actuators with Different Orientation Angles Using Echo State Networks for Irregular Time Series Data," *Micromachines (Basel)*, vol. 13, no. 2, p. 216, Jan. 2022, doi: 10.3390/mi13020216.
- [21] D. Drotman, M. Ishida, S. Jadhav, and M. T. Tolley, "Application-Driven Design of Soft, 3-D Printed, Pneumatic Actuators with Bellows," *IEEE/ASME Transactions on Mechatronics*, vol. 24, no. 1, pp. 78–87, Feb. 2019, doi: 10.1109/TMECH.2018.2879299.
- [22] Y. Elsayed et al., "Finite element analysis and design optimization of a pneumatically actuating silicone module for robotic surgery applications", *Soft Robot*. DOI:10.1089/soro.2014.0016
- [23] Elango, N.; Faudzi, A. A review article: Investigations on soft materials for soft robot manipulations. *Int. J. Adv. Manuf. Technol.* 2015, 80, 1027–1037
- [24] P. Polygerinos et al., "Modeling of Soft Fiber-Reinforced Bending Actuators," in *IEEE Transactions on Robotics*, vol. 31, no. 3, pp. 778-789, June 2015, doi: 10.1109/TRO.2015.2428504.
- [25] H. Zhang, A. S. Kumar, F. Chen, J. Y. H. Fuh and M. Y. Wang, "Topology Optimized Multimaterial Soft Fingers for Applications on Grippers, Rehabilitation, and Artificial Hands," in *IEEE/ASME Transactions on Mechatronics*, vol. 24, no. 1, pp. 120-131, Feb. 2019, doi: 10.1109/TMECH.2018.2874067.
- [26] P. Glick, S. A. Suresh, D. Ruffatto, M. Cutkosky, M. T. Tolley, and A. Parness, "A Soft Robotic Gripper with Gecko-Inspired Adhesive," *IEEE Robot Autom Lett*, vol. 3, no. 2, pp. 903–910, Apr. 2018, doi: 10.1109/LRA.2018.2792688.
- [27] Kuriyama, M.; Takayama, T. 2-DOF Woven Tube Plane Surface Soft Actuator Using Extensional Pneumatic Artificial Muscle. *Hardware* 2024, 2, 50-6 <https://doi.org/10.3390/hardware2010003>
- [28] R. V. Martinez, C. R. Fish, X. Chen and G. M. Whitesides, "Elastomeric origami: Programmable paper-elastomer composites as pneumatic actuators", *Adv.*

- [29] Manns, M.; Morales, J.; Frohn, P. Additive manufacturing of silicon based PneuNets as soft robotic actuators. *Procedia CIRP* 2018, 72, 328–333.
- [30] Ei Cho S, Chenette EJ (2024) Improving the diversity of the PLOS ONE editorial board. *PLoS ONE* 19(8): e0308492. <https://doi.org/10.1371/journal.pone.0308492>
- [31] M. Soliman, M. A. Saleh, M. A. Mousa, M. Elsamanty, and A. G. Radwan, “Theoretical and experimental investigation study of data driven work envelope modelling for 3D printed soft pneumatic actuators,” *Sens Actuators A Phys*, vol. 331, p. 112978, Nov. 2021, doi: 10.1016/j.sna.2021.112978.
- [32] Jiang, Z.; Wang, Y.; Zhang, K. Development of a Pneumatically Actuated Quadruped Robot Using Soft–Rigid Hybrid Rotary Joints. *Robotics* 2024, 13, 24 <https://doi.org/10.3390/robotics13020024>
- [33] G. Bao et al., “Soft robotics: Academic insights and perspectives through bibliometric analysis,” *Soft Robot*, vol. 5, no. 3, pp. 229–241, 2018, doi: 10.1089/soro.2017.0135.
- [34] J. Liu, Z. Ma, Y. Wang and S. Zuo, "Reconfigurable Self-Sensing Pneumatic Artificial Muscle With Locking Ability Based on Modular Multi-Chamber Soft Actuator," in *IEEE Robotics and Automation Letters*, vol. 7, no. 4, pp. 8635-8642, Oct. 2022, doi: 10.1109/LRA.2022.3189154.
- [35] Y. Yang and Y. Chen, “Innovative Design of Embedded Pressure and Position Sensors for Soft Actuators,” *IEEE Robot Autom Lett*, vol. 3, no. 2, pp. 656–663, Apr. 2018, doi: 10.1109/LRA.2017.2779542.
- [36] H. A. Elkholy, A. S. Shahin, A. W. Shaarawy, H. Marzouk, and M. Elsamanty, “Solving Inverse Kinematics of a 7-DOF Manipulator Using Convolutional Neural Network,” 2020, pp. 343–352. doi: 10.1007/978-3-030-44289-7_32.
- [37] F. Yang et al., “Design and Optimize of a Novel Segmented Soft Pneumatic Actuator,” *IEEE Access*, vol. 8, pp. 122304–122313, 2020, doi: 10.1109/ACCESS.2020.3006865
- [38] J. Huang, Y. Cao, C. Xiong and H. -T. Zhang, "An Echo State Gaussian Process-Based Nonlinear Model Predictive Control for Pneumatic Muscle Actuators," in *IEEE Transactions on Automation Science and Engineering*, vol. 16, no. 3, pp. 1071-1084, July 2019, doi: 10.1109/TASE.2018.2867939.